HHS Public Access

Author manuscript

Procedia Manuf. Author manuscript; available in PMC 2021 May 17.

Published in final edited form as:

Procedia Manuf. 2019 ; 34: 247–251. doi:10.1016/j.promfg.2019.06.146.

Manufacturing and Characterization of Zn-WC as Potential Biodegradable Material

Zeyi Guan[a], **Shuaihang Pan**[a], **Chase Linsley**[b], **Xiaochun Li**[a,c,*]

[a]University of California, Los Angeles, 405 Westwood plaza, Los Angeles, Department of Mechanical and Aerospace Engineering, School of Engineering, 90095 USA

[b]University of California, Los Angeles, 405 Westwood plaza, Los Angeles, Department of Bioengineering, School of Engineering, 90095 USA

[c]University of California, Los Angeles, 405 Westwood plaza, Los Angeles, Department of Material Science and Engineering, School of Engineering, 90095 USA

Abstract

This work presents the manufacturing and characterization of zinc-tungsten carbide (Zn-WC) nanocomposite as a potential biodegradable material. A highly homogeneous WC nanoparticle dispersion in a Zn matrix was achieved by molten salt assisted stir casting followed with hot rolling. The Vickers microhardness and ultimate tensile strength of zinc were enhanced more than 50% and 87%, respectively, with the incorporation of up to 4.4 vol. % WC nanoparticles. Additionally, Zn-WC nanocomposite retained high ductility (> 65%). However, the electrical and thermal conductivities were reduced by 12% and 21%, respectively. The significant enhancement in mechanical strength makes nanoparticle-reinforced zinc a promising candidate material for biodegradable metallic implants for a wide range of clinical applications, including orthopaedic and cardiovascular implants as well as bioresorbable electronics.

Keywords

Metal matrix nanocomposite; zinc; biodegradable metal; bioresorbable stent; stength and ductility

1. Introduction

Metallic implants are the gold standard for clinical applications requiring high strength-to-bulk ratio (e.g. bone fixation screws/pins, cardiovascular stents, etc.). However, many clinical indications only need temporary support while the tissue heals. Metallic implants made of biomaterials like titanium (Ti) alloys [1], stainless steel [2] and cobalt-chromium (Co-Cr) alloys [3] are permanent, and either require a second surgery to remove or they remain in the body where there is a risk for long-term complications (e.g. inflammation, tissue loss, etc.). Conversely, biodegradable materials including zinc (Zn), magnesium (Mg)

*Corresponding author. Tel.: +1-310-825-2383. xcli@seas.ucla.edu.

[4], iron (Fe) [5], and some biodegradable polymers [6] provide the required support during healing and then progressively degrade after completing its function. For high-stress applications, biodegradable metals are the ideal choice because of their mechanical strength and stiffness. Mg has been the most studied biodegradable metal because of its reasonable mechanical strength and proven biocompatibility. However, there are limitations to Mg, namely the rapid corrosion rate, high hydrogen evolution *in-vivo* [7], and chronic inflammation has been observed in tissue surrounding Mg implants [8].

In the last decade, Zn has been studied as an alternative to Mg. Zn has excellent biocompatibility [9] and has already shown great potential in biotech applications, ranging from electrodes for batteries [10] and sensors [11] to micro/nanofillers for conductive paste [12] as the filament or alloying element. This is because the electrical conductivity of Zn is much higher than most of the biocompatible semiconductors, making Zn a suitable option for bioresorbable electronics. However, its success as a structural material is limited because of its low mechanical strength and modulus. This is unfortunate because recent studies have evaluated Zn has a potential material for bioresorbable stents (BRS) and found that Zn offers an ideal corrosion rate (10um/year) that would allow vascular healing to occur before the stent biodegraded. Additionally, no inflammation was observed in arteries containing a Zn implant [13]. Despite these promising results, no commercially available Zn-based BRS are commercially available. Enhancing the strength of Zn would make is an ideal candidate for clinical applications requiring implants designed to withstand high stresses. Alloying has been one of the most popular methods to strengthen Zn by using a low concentration of a second metal element. The mechanisms mainly depend on intermetallic phase precipitation strengthening and solid solution strengthening [14]. However, this can negatively impact Zn's corrosion rate, as well as reduce the ductility. Furthermore, depending on the alloying element(s) used, biocompatibility could also be compromised.

Nanoparticles have been reported as an effective method for mechanical strengthening in metallic materials due to the precipitation strengthening (Orowan strengthening), grain refinement (Hall-Petch effect) and load bearing [15]. Moreover, by using chemically and thermally stable nanoparticles [16], Zn matrix nanocomposite could achieve the balance among biocompatibility, corrosion rate, and ductility. However, the grand challenge of metal matrix nanocomposite manufacturing is the nanoparticle dispersion problem, where agglomeration and sintering would generate defects and cracks. Therefore, in this study, we demonstrate the manufacturing method of high-performance Zn-WC nanocomposite with uniform nanoparticle dispersion according to the nanoparticle self-dispersion mechanism [15] and the characterization results of strong and ductile Zn-WC nanocomposite as a potential biodegradable material. WC nanoparticles were mainly utilized to enhance the mechanical strength of Zn. Zn-WC nanocomposites obtained an overall optimized combination of mechanical properties and physical properties, serving as an ideal biodegradable material. This study has also investigated the thermal/electrical conductivity of Zn-WC nanocomposite, to validate the viability of being used in bioelectronics.

2. Method

Salt assisted stir casting was performed to mass produce Zn-WC nanocomposite, which has recently been demonstrated to be an efficient method for other composite systems [17, 18]. An induction finance was used to melt potassium aluminum fluoride ($KAlF_4$) at 700°C in a 3kg-capacity graphite crucible (89mm in height and 130mm in inner diameter). This molten salt was used for surface oxidation removal. Bulk Zn (99.9%, RotoMetals) was weighed and added to the crucible. The molten salt was used to cover the metal and protect it from oxidation. WC nanoparticles (50–200nm) were mixed with fine $KAlF_4$ salt powders at a volume ratio of 1:20. This powder mixture was slowly added to the crucible until 5 vol.% and 10 vol.% WC nanoparticles concentration was reached. A graphite stirrer set to 400 rpm was used to mix and incorporate the WC nanoparticles (1.0 hour). The top layer of low-density molten salt was removed prior to casting Zn-WC to a 2-inch diameter disk with a 0.4-inch thickness. Hot rolling of the Zn-WC nanocomposite was performed at 200°C with a thickness reduction ratio of 1:7. Thin plates (0.06-inch thickness) were used for microstructure characterization by scanning electron microscopy (SEM), element detection by x-ray diffraction (XRD) and inductively coupled plasma mass spectrometry (ICP-MS), and electrical/ thermal conductivity measurement. Wire-electrical discharge machining (wire-EDM) was used to cut samples to dog-bone shape for the tensile test (tensile test standard shown in Table 1).

3. Characterization

3.1. WC concentration

To accurately measure nanoparticle concentrations and account for any dispersion inhomogeneity, ICP-MS was used to measure metallic element concentrations. Briefly, Zn-WC nanocomposites were ground to small pieces, and aqua regia was used to extract elemental W. The results were converted to WC concentrations in volume percentage, shown in Table 2. In this study, Zn-WC nanocomposite samples had lower than designed due to poor nanoparticle incorporation efficiency during manufacturing. The final Zn-WC nanocomposite formulations were Zn-2.6 vol.% WC and Zn-4.4 vol.% WC, which were characterized and compared to pure Zn samples processed under the same conditions.

3.2. Chemical composition

XRD was performed on the nanocomposite samples and the reference sample to semi-quantitively characterize the chemical composition on the surfaces of the materials, shown in Fig.1. The diffraction peaks of WC could be observed on the XRD pattern for Zn-2.6WC and Zn-4.4WC samples, where the diffraction angles are from 30 to 90 degrees. Furthermore, no unwanted by-products were observed, indicating that WC nanoparticle did not react with Zn during manufacturing and processing.

3.3. Microstructures

SEM in backscattering mode was performed on the nanocomposite samples to investigate the nanoparticle dispersion, shown in Fig.2. The bright phase represents the WC nanoparticles, while the darker phase represents the Zn matrix. Compared with Zn-2.6WC

(Fig. 2(a) and 2(b)), which obtained zones of dense nanoparticles, Zn-4.4WC (Fig. 2(c) and 2(d)) achieved better homogeneity. To investigate the impact that nanoparticles have on the crystal structure, optical images were shown in Fig. 2e–g, where hot rolled samples were etched (etchant: 20% CrO_3 and 5% Na_2SO_4 in distilled water). The grain size reduced from 17.4um to 6.1um for 4.4% WC nanoparticle incorporation (Fig. 2h).

3.4. Hardness and mechanical properties from tensile test

The grain-size effect on the mechanical properties (Hall-Petch effect) was evaluated using Vickers microhardness testing and tensile testing. Microhardness was measured using 300gf and 10s dwelling time. Fig. 3(a) shows that Vickers microhardness of the Zn-4.4%WC nanocomposite has increased by more than 43% from 34.9HV to 55.0HV. Tensile testing was performed using an Instron 5966 Dual Column Tabletop Testing system. The results show the ultimate tensile strength (UTS) of Zn-4.4WC increased by 87% from 89.1 MPa to 166.3 MPa, while the ductility only decreased from 70.1% to 65.1% (Fig. 3(b) and Table 3). These results show that homogeneous nanoparticle dispersion could be used to avoid significant ductility reduction, which has been reported by a previous study on metal matrix nanocomposites [19].

3.5. Electrical conductivity and thermal conductivity

The sheet resistance of nanocomposite samples was measured by *ResMap four-point probe* (Fig. 4(a)), and thermal conductivity was calculated using heat capacity measurements from differential scanning calorimetry (DSC) and thermal diffusivity by laser flash analysis (Fig. 4(b)). The electrical conductivity decreased from 10.2×10^6 S/m to 8.9×10^6 S/m for Zn-4.4WC, and the thermal conductivity decreased from 114.6 W/m-K to 91.0 W/m-K. According to one-way ANOVA analysis, electrical conductivity and thermal conductivity have p values of 5.5% and 7.0%, respectively, indicating that no significant reduction after nanoparticle incorporation. All related mechanical and physical results are presented in Table 4.

4. Discussion

Good wettability between WC and molten Zn enables a self-stabilization mechanism through a force balance between the particle-particle van der Waals force and the particle-molten metal surface tension [15]. This produces a nanoparticle self-dispersion within the molten Zn. However, when the nanoparticle size is not small enough, pseudo self-dispersion occurs, where there is a favorable particle-particle distance (e.g. approximately a few nanometers in Zn-WC system). Thus, pseudo-microcluster was observed in Zn-2.6WC. Zn-4.4WC, on the other hand, obtained a much better nanoparticle dispersion due to the higher concentration. The problem of non-uniform dispersion could be solved by using smaller sized nanoparticles.

The major strengthening mechanisms of the Zn-WC nanocomposite are grain refinement and precipitation hardening. Zinc's grain size is one of the determinant factors for mechanical strength. For instance, cast zinc with 100μm grain size only has a UTS of 30MPa. The nanoparticle-induced grain refinement achieved in this study is due to grain

growth impedance during solidification. The finer crystalline structure (6.1μm grain size) enables grain-boundary strengthening, also known as Hall-Petch strengthening, by impeding dislocation propagation. Another contributor to the increased mechanical strength is the precipitation strengthening effect directly from WC nanoparticles. The nanoparticles presence blocks dislocation movement, which means dislocations need higher energy to shear through/around the nanoparticles (i.e. Orowan mechanism) [20]. Other strengthening mechanisms that may apply but are not dominant in this case include load-transfer effect and thermal expansion coefficient/elastic modulus mismatch.

Previous studies on nanoparticle reinforced metal matrix nanocomposites reported that this strategy negatively impacted ductility because of nanoparticle agglomeration, sintering, impurities, and voids. Such defects can cause premature fracture through crack propagation during tensile testing. In this study, salt assisted stir casting protected against the formation of these defects by preventing zinc oxide contamination, nanoparticle agglomeration and sintering. A good nanoparticle dispersion was achieved by self-stabilization mechanism, and hot extrusion processing could further enhance the dispersion homogeneity by allowing nanoparticles migration [21].

The Zn-WC nanocomposites successfully manufactured in this study could be used to create the next generation of bioresorbable electronics and metallic implants. Zn [22, 23] and WC [24] have both been previously shown to be non-toxic. The Zn-WC nanocomposites studied in this research have shown a good combination of material properties, including mechanical ductility (elongation to failure > 65%), mechanical strength (UTS ~ 166.3MPa, YS ~126.9MPa), microhardness (~55HV), electrical conductivity (8.9×10^6 S/m) thermal conductivity (~91W/m-K). The enhanced mechanical properties provide the strength bioresorbable devices require to withstand physiological forces. For example, the combination of high mechanical strength and high ductility makes Zn-WC nanocomposites a promising material choice for BRS designed for high-stress applications (e.g. aortic stenting). The high electrical conductivity provides a better signal-to-noise ratio in sensing and high thermal conductivity provides faster heat release for electronics. With an optimized combination of good toughness and electrical/thermal conductivity, Zn-WC nanocomposite would be suitable for applications such as electrodes and interconnects in bioresorbable electronics [11].

5. Conclusion

This study presents a successful manufacturing process, molten salt assisted stir casting, for novel Zn-4.4WC nanocomposite with highly homogeneous nanoparticle dispersion. Characterization of the resulting nanocomposites found that a combination of good mechanical properties (UTS ~ 166.3MPa, ultimate strain >65%) and physical properties (no significant reduction on electrical/thermal properties) had been achieved with only 4.4% WC nanoparticles added to the Zn matrix. The results from this study show that Zn-WC nanocomposites could be a promising material for load-bearing biodegradable metallic implants and bioresorbable electronics.

Future studies will investigate the impact that nanoparticle size, shape and concentration have on the material properties. This will allow for the fabrication of nanocomposites with material properties that match the application requirements. Also, it will be essential to investigate the corrosion behavior of the novel Zn nanocomposite material. Additionally, Zn-based materials have a limited shelf life due to Zn's low recrystallization temperature, which causes self-annealing and decreased mechanical properties over time. Further investigation is needed to study how nanoparticles impact Zn's recrystallization process and the subsequent impact on long-term mechanical stability.

Acknowledgments

This work is partially supported by The National Science Foundation (NSF) under the Grant No. CMMI #1449395.

References

[1]. Gepreel MA-H, Niinomi M, Biocompatibility of Ti-alloys for long-term implantation, Journal of the mechanical behavior of biomedical materials, 20 (2013) 407–415. [PubMed: 23507261]

[2]. Subramanian B, Ananthakumar R, Kobayashi A, Jayachandran M, Surface modification of 316L stainless steel with magnetron sputtered TiN/VN nanoscale multilayers for bio implant applications, Journal of Materials Science: Materials in Medicine, 23 (2012) 329–338. [PubMed: 22113251]

[3]. Rodrigues WC, Broilo LR, Schaeffer L, Knörnschild G, Espinoza FRM, Powder metallurgical processing of Co–28% Cr–6% Mo for dental implants: Physical, mechanical and electrochemical properties, Powder Technology, 206 (2011) 233–238.

[4]. Virtanen S, Biodegradable Mg and Mg alloys: Corrosion and biocompatibility, Materials Science and Engineering: B, 176 (2011) 1600–1608.

[5]. Lin W, Qin L, Qi H, Zhang D, Zhang G, Gao R, Qiu H, Xia Y, Cao P, Wang X, Long-term in vivo corrosion behavior, biocompatibility and bioresorption mechanism of a bioresorbable nitrided iron scaffold, Acta biomaterialia, 54 (2017) 454–468. [PubMed: 28315492]

[6]. Nair LS, Laurencin CT, Biodegradable polymers as biomaterials, Progress in polymer science, 32 (2007) 762–798.

[7]. Aghion E, Levy G, Ovadia S, In vivo behavior of biodegradable Mg– Nd–Y–Zr–Ca alloy, Journal of Materials Science: Materials in Medicine, 23 (2012) 805–812. [PubMed: 22190200]

[8]. Witte F, Ulrich H, Rudert M, Willbold E, Biodegradable magnesium scaffolds: Part 1: appropriate inflammatory response, Journal of biomedical materials research Part A, 81 (2007) 748–756. [PubMed: 17390368]

[9]. Bowen PK, Drelich J, Goldman J, Zinc exhibits ideal physiological corrosion behavior for bioabsorbable stents, Advanced materials, 25 (2013) 2577–2582. [PubMed: 23495090]

[10]. Li S, Guo ZP, Wang CY, Wallace GG, Liu HK, Flexible cellulose based polypyrrole–multiwalled carbon nanotube films for bio-compatible zinc batteries activated by simulated body fluids, Journal of Materials Chemistry A, 1 (2013) 14300–14305.

[11]. Shou W, Mahajan BK, Ludwig B, Yu X, Staggs J, Huang X, Pan H, Low - Cost Manufacturing of Bioresorbable Conductors by Evaporation–Condensation-Mediated Laser Printing and Sintering of Zn Nanoparticles, Advanced Materials, 29 (2017) 1700172.

[12]. Li J, Luo S, Liu J, Xu H, Huang X, Processing Techniques for Bioresorbable Nanoparticles in Fabricating Flexible Conductive Interconnects, Materials, 11 (2018) 1102.

[13]. Guillory RJ, Bowen PK, Hopkins SP, Shearier ER, Earley EJ, Gillette AA, Aghion E, Bocks M, Drelich JW, Goldman J, Corrosion characteristics dictate the long-term inflammatory profile of degradable zinc arterial implants, ACS Biomaterials Science & Engineering, 2 (2016) 2355–2364.

[14]. Jin H, Zhao S, Guillory R, Bowen PK, Yin Z, Griebel A, Schaffer J, Earley EJ, Goldman J, Drelich JW, Novel high-strength, low-alloys Zn-Mg (< 0.1 wt% Mg) and their arterial biodegradation, Materials Science and Engineering: C, 84 (2018) 67–79. [PubMed: 29519445]

[15]. Chen L-Y, Xu J-Q, Choi H, Pozuelo M, Ma X, Bhowmick S, Yang J-M, Mathaudhu S, Li X-C, Processing and properties of magnesium containing a dense uniform dispersion of nanoparticles, Nature, 528 (2015) 539–543. [PubMed: 26701055]

[16]. Armstead AL, Arena CB, Li BY, Exploring the potential role of tungsten carbide cobalt (WC-Co) nanoparticle internalization in observed toxicity toward lung epithelial cells in vitro, Toxicology and Applied Pharmacology, 278 (2014) 1–8. [PubMed: 24746988]

[17]. Guan Z, Hwang I, Pan S, Li X, Scalable Manufacturing of AgCu^ 40 (wt.%)-WC Nanocomposite Microwires, Journal of Micro and Nano-Manufacturing, (2018).

[18]. Liu W, Cao C, Xu J, Wang X, Li X, Molten salt assisted solidification nanoprocessing of Al-TiC nanocomposites, Materials Letters, 185 (2016) 392–395.

[19]. Saheb N, Iqbal Z, Khalil A, Hakeem AS, Al Aqeeli N, Laoui T, Al-Qutub A, Kirchner R, Spark plasma sintering of metals and metal matrix nanocomposites: a review, Journal of Nanomaterials, 2012 (2012) 18.

[20]. Casati R, Aluminum matrix composites reinforced with alumina nanoparticles, Springer, 2016.

[21]. Choi H, Alba-Baena N, Nimityongskul S, Jones M, Wood T, Sahoo M, Lakes R, Kou S, Li X, Characterization of hot extruded Mg/SiC nanocomposites fabricated by casting, Journal of materials science, 46 (2011) 2991–2997.

[22]. Bowen PK, Guillory II RJ, Shearier ER, Seitz J-M, Drelich J, Bocks M, Zhao F, Goldman J, Metallic zinc exhibits optimal biocompatibility for bioabsorbable endovascular stents, Materials Science and Engineering: C, 56 (2015) 467–472. [PubMed: 26249616]

[23]. Nriagu J, Zinc toxicity in humans, School of Public Health, University of Michigan, (2007).

[24]. Bastian S, Busch W, Kühnel D, Springer A, Meißner T, Holke R, Scholz S, Iwe M, Pompe W, Gelinsky M, Toxicity of tungsten carbide and cobalt-doped tungsten carbide nanoparticles in mammalian cells in vitro, in, National Institute of Environmental Health Sciences, 2008.

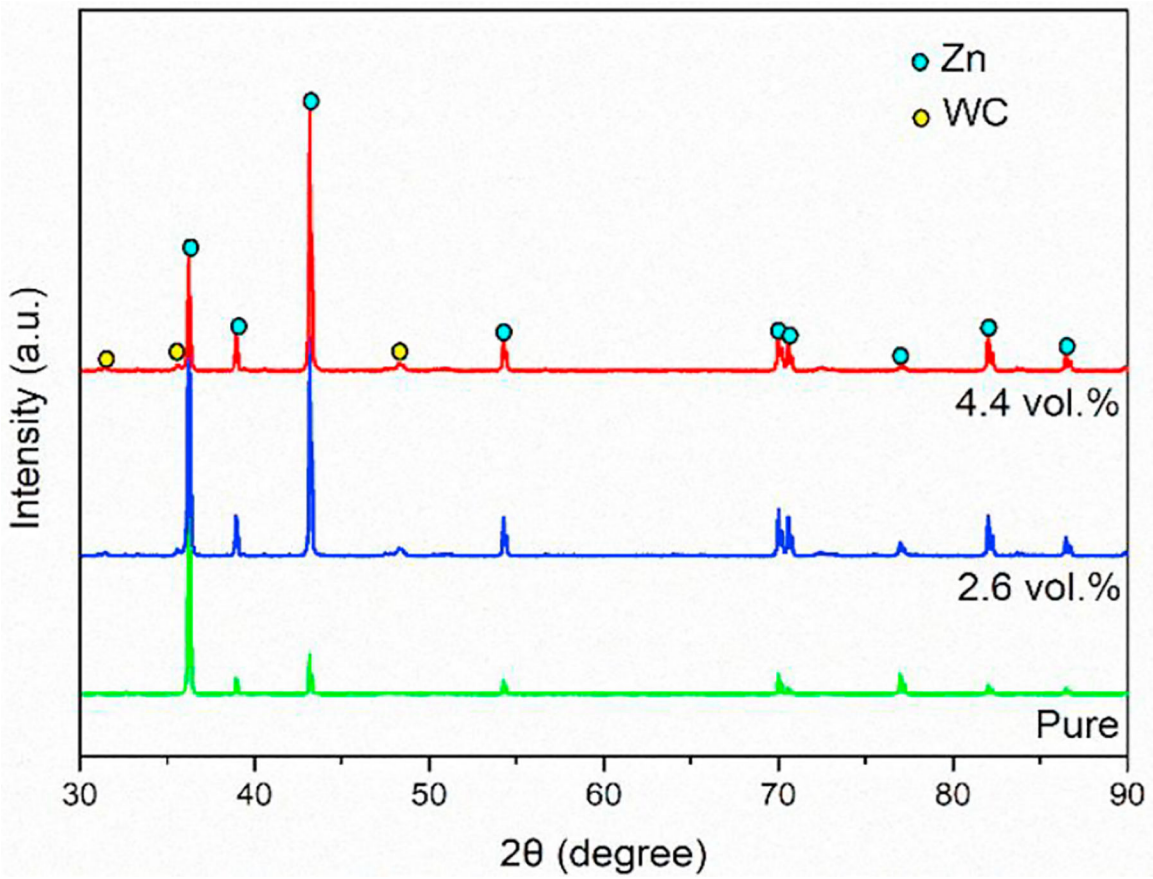

Fig. 1.
Diffraction pattern of Zn and Zn-WC nanocomposite samples.

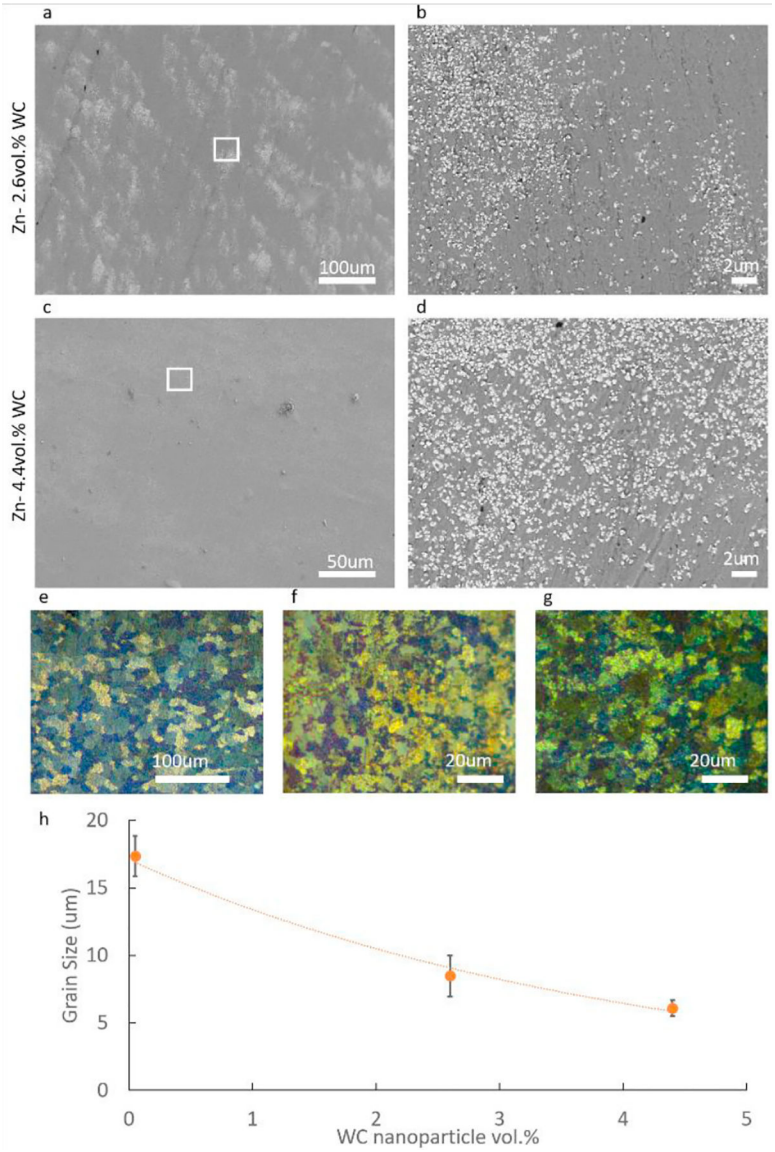

Fig 2.

Zn-WC nanocomposite microstructure from SEM in back scattering mode. (a) and (c) represent Zn-2.6 vol.% WC sample and Zn-4.4 vol.% WC sample, while (b) and (d) are the magnified images. Optical images of hot-rolled sample for grain size measurement, including (e) Zn, (f) Zn-2.6WC and (g) Zn-4.4WC. (d) shows the grain size refinement effect with respect to the nanoparticle concentration.

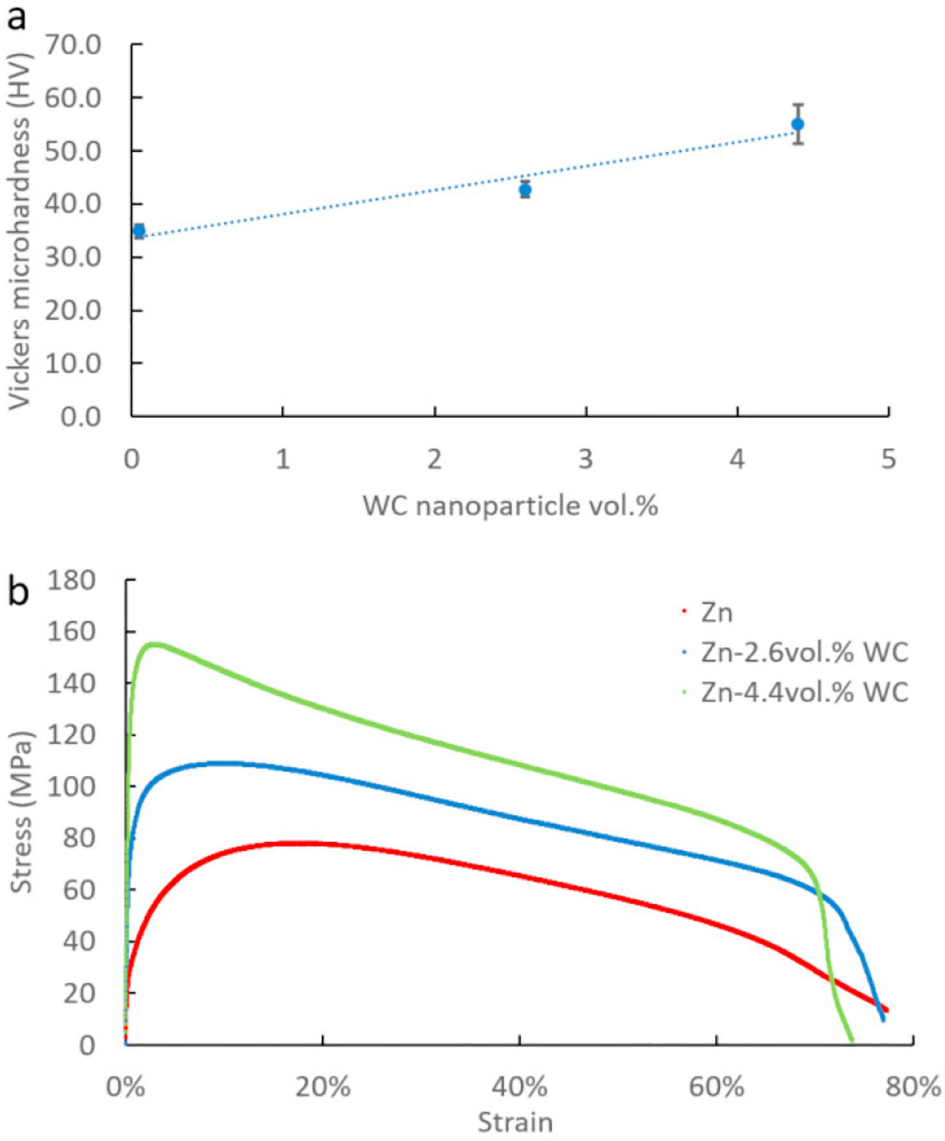

Fig. 3.

(a) Vickers microhardness Zn-WC nanocomposite samples; (b) Stress-strain curves of the Zn and Zn-WC nanocomposite samples from tensile test.

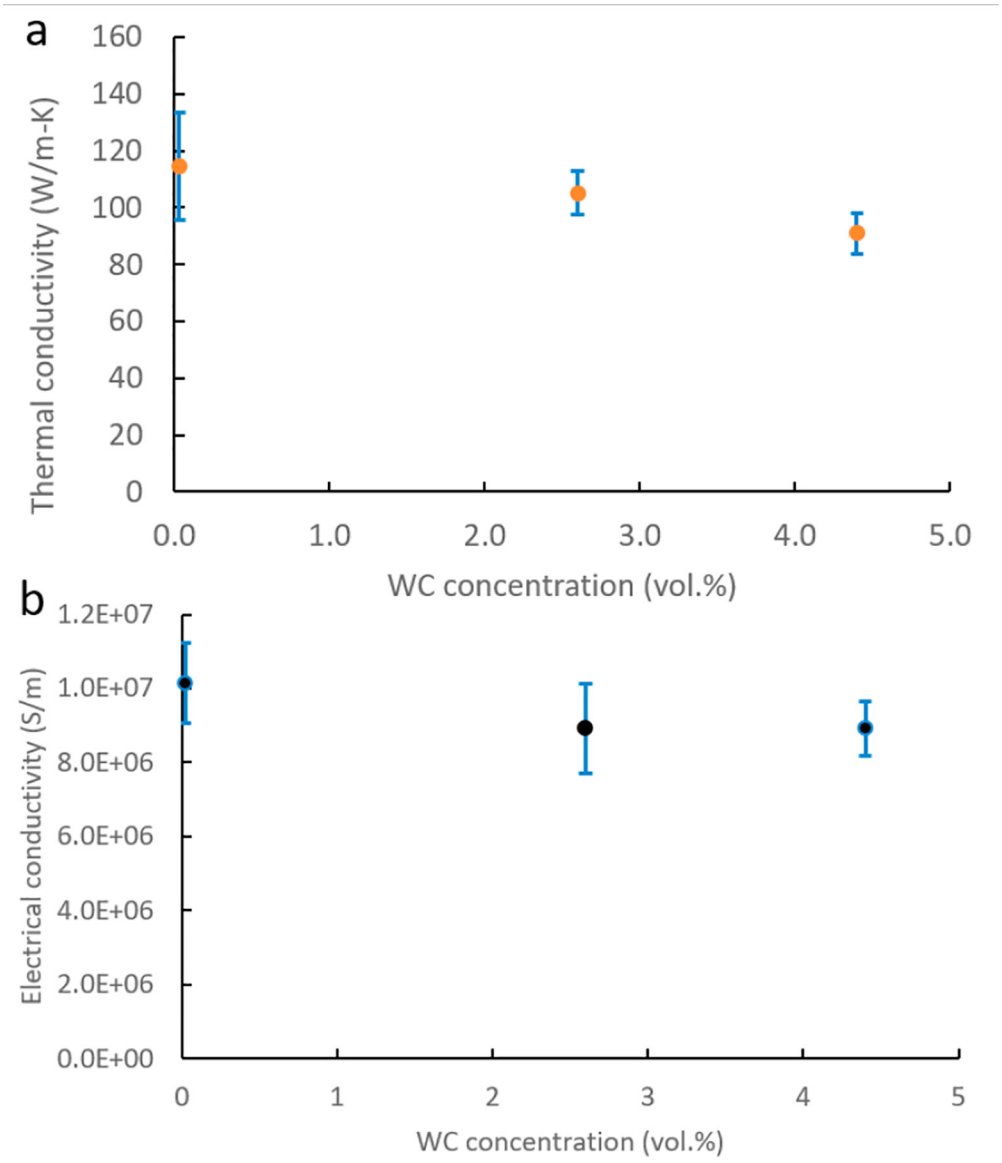

Fig. 4.

(a) Thermal conductivity of Zn-WC with respect to the WC nanoparticle concentration; (b) electrical conductivity of Zn-WC with respect to the WC nanoparticle concentration.

Table 1:

Tensile test standard

Standard	**ASTM E8/E8M**
Shape	Rectangular subsize specimen
Width	6mm
Gauge length	25mm
Strain rate	0.5mm/min

Table 2.

ICP-MS result of Zn and Zn-WC nanocomposite samples (10mg per sample and 3 tests were performed on each sample)

	Concentration [mg/g]		
	Zn	**W**	**WC (vol.%)**
Zn	769.2±4.5	1.2±0.0	0.0
Zn-2.6 WC	761.4±1.7	42.0±1.5	2.6
Zn-4.4 WC	802.7±0.2	75.8±2.3	4.4

Table 3.

Tensile test results of ASTM subsize dog bone shape samples

	UTS (MPa) Yield	strength (MPa)	Elongation to fail
Zn	89.1±15.4	35.6±10.4	70.1±10.2%
Zn-2.6WC	111.6±3.4	75.1±8.8	69.7±10.3%
Zn-4.4WC	166.3±15.7	126.9±2.7	65.1±12.3%

Table 4.

Physical properties of hot-rolled Zn/Zn nanocomposite plate

	Grain size (μm)	Vickers microhardne ss (HV)	Electrical conductivity (X10^6 S/m)	Thermal conductivity (W/m-K)
Zn	17.4±1.5	34.9±1.2	10.2±1.1	114.6±19.0
Zn-2.6WC	8.5±1.5	42.7±1.5	8.9±1.2	105.2±7.8
Zn-4.4WC	6.1±0.6	55.0±3.6	8.9±0.7	91.0±7.2